

## Scaling of forced magnetic reconnection in the Hall-magnetohydrodynamical Taylor problem with arbitrary guide field

Richard Fitzpatrick

Citation: *Physics of Plasmas* (1994-present) **11**, 3961 (2004); doi: 10.1063/1.1768956

View online: <http://dx.doi.org/10.1063/1.1768956>

View Table of Contents: <http://scitation.aip.org/content/aip/journal/pop/11/8?ver=pdfcov>

Published by the [AIP Publishing](#)

---

### Articles you may be interested in

[Nonlinear effects on magnetic energy release by forced magnetic reconnection: Long wavelength perturbations](#)  
*Phys. Plasmas* **13**, 052902 (2006); 10.1063/1.2200630

[Solar coronal heating by forced magnetic reconnection: Multiple reconnection events](#)  
*Phys. Plasmas* **12**, 012904 (2005); 10.1063/1.1831278

[Forced magnetic reconnection in the inviscid Taylor problem](#)  
*Phys. Plasmas* **11**, 3525 (2004); 10.1063/1.1756587

[Scaling of forced magnetic reconnection in the Hall-magnetohydrodynamic Taylor problem](#)  
*Phys. Plasmas* **11**, 937 (2004); 10.1063/1.1640378

[A numerical study of forced magnetic reconnection in the viscous Taylor problem](#)  
*Phys. Plasmas* **10**, 2304 (2003); 10.1063/1.1574516

---



# Scaling of forced magnetic reconnection in the Hall-magnetohydrodynamical Taylor problem with arbitrary guide field

Richard Fitzpatrick<sup>a)</sup>

Center for Magnetic Reconnection Studies, Institute for Fusion Studies, Department of Physics,  
University of Texas at Austin, Austin, Texas 78712

(Received 12 February 2004; accepted 14 May 2004; published online 12 July 2004)

Two-dimensional, nonlinear, Hall-magnetohydrodynamical (MHD) numerical simulations are used to investigate the scaling of the rate of forced magnetic reconnection in the so-called Taylor problem. In this problem, a small amplitude boundary perturbation is suddenly applied to a tearing stable, slab plasma equilibrium. The perturbation is such as to drive magnetic reconnection within the plasma. This type of reconnection, which is not due to an intrinsic plasma instability, is generally termed “forced reconnection.” Hall effects are found to greatly accelerate the rate of magnetic reconnection, relative to the well-known Sweet–Parker rate. In the nonlinear Hall-MHD regime with arbitrary guide field, the peak reconnection rate is found to be independent of the resistivity, and to scale like  $d\psi/dt \sim [\beta/(1+\beta)]^{3/4} d_i^{3/2} \Xi_0^2$ , where  $\beta$  is the plasma beta calculated using the guide field,  $d_i$  the collisionless ion skin depth, and  $\Xi_0$  the amplitude of the boundary perturbation. © 2004 American Institute of Physics. [DOI: 10.1063/1.1768956]

## I. INTRODUCTION

Magnetic reconnection is a phenomenon which occurs in a wide variety of laboratory and space plasmas, e.g., magnetic fusion experiments,<sup>1</sup> the solar corona,<sup>2</sup> and the Earth’s magnetotail.<sup>3</sup> The reconnection process gives rise to a change in magnetic-field-line topology with an accompanying release of magnetic energy and acceleration of charged particles. Conventional resistive-magnetohydrodynamical (MHD) theory is capable of accounting for magnetic reconnection, but generally predicts reconnection rates which are many orders of magnitude smaller than those observed.<sup>4</sup> On the other hand, more sophisticated plasma models which treat electrons and ions as separate fluids yield much faster reconnection rates which are fairly consistent with observations.<sup>5,6</sup>

At this stage, it is helpful to make a few definitions. Let  $d_i = c/\omega_{pi}$  and  $d_e = c/\omega_{pe} \ll d_i$  be the ion and electron collisionless skin depths, respectively. Suppose that  $\delta$  is the width of the reconnecting layer and is determined by resistivity. A conventional resistive-MHD treatment of the plasma is appropriate when  $\delta \gg d_i$ . In this model, the ions and electrons move together as a single fluid. A Hall-MHD treatment of the plasma is appropriate when  $d_e \ll \delta \ll d_i$ . In this model, the ion and electron motions decouple on length scales below  $d_i$ . In fact, the only difference between Hall MHD and resistive MHD is the presence of the Hall term in Ohm’s law in the former case. Note that electron inertia can be safely neglected in the Hall-MHD model provided that  $\delta \gg d_e$ .

This paper investigates a model two-dimensional (2D) magnetic reconnection problem which was first proposed by Taylor. In this problem, a stable, slab plasma equilibrium with a central magnetic-field resonance is subject to a suddenly imposed, small amplitude boundary perturbation

which is such as to drive magnetic reconnection at the resonance. This type of reconnection, which is not due to an intrinsic plasma instability, is generally termed “forced reconnection.”

The so-called “Taylor problem” has already been thoroughly investigated within the context of resistive MHD.<sup>7–9</sup> Furthermore, a recent numerical investigation of this problem<sup>10</sup> using Hall-MHD equations in the low “guide field” (i.e., equilibrium magnetic field directed perpendicular to the reconnecting field) and cold ion limit has established the following scaling law for the maximum nonlinear reconnection rate:

$$R_{\max} \sim d_i^{3/2} \Xi_0^2, \quad (1)$$

where  $d_i$  is the collisionless ion skin depth and  $\Xi_0$  the amplitude of the boundary perturbation. The above nonlinear reconnection rate is generally much faster than that obtained from resistive MHD, i.e.,<sup>8</sup>

$$R_{\max} \sim \eta^{1/2} \Xi_0^{3/2}, \quad (2)$$

where  $\eta$  is the resistivity. Incidentally, the above expression corresponds to the well-known Sweet–Parker reconnection rate.<sup>11,12</sup> Note, in particular, that in expression (1) there is *no dependence* on the mechanism by which magnetic-field lines are broken (i.e., on the resistivity). This result is consistent with earlier numerical studies of two-fluid magnetic reconnection in the low guide-field limit (see Refs. 13 and 14, and references therein) which have established that the reconnection rate is accelerated above the resistive-MHD rate through the action of the *whistler wave*, is independent of the mechanism by which magnetic-field lines are broken, and is controlled by the ion dynamics. There remains, however, some debate as to the exact dependence of the nonlinear reconnection rate on the collisionless ion skin depth  $d_i$ . Wang, Bhat-tacharjee, and Ma<sup>15</sup> report a  $d_i^{1/2}$  scaling, both Fitzpatrick<sup>10</sup>

<sup>a)</sup>Electronic address: rfitzp@farside.ph.utexas.edu

and Matthaeus<sup>16</sup> report a  $d_i^{3/2}$  scaling, whereas Shay *et al.*<sup>17</sup> find no (direct) scaling with  $d_i$ . Recently, Shay *et al.*<sup>18</sup> have suggested that all the aforementioned  $d_i$  scalings can be accounted for in terms of a unified theory in which the plasma inflow rate is fixed at  $\approx 0.1$  of the Alfvén velocity calculated using the “upstream magnetic-field strength.” The upstream field strength is defined as the reconnecting field strength at the edge of the “dissipation region,” i.e., the region, centered on the resonant surface, where resistive MHD breaks down and the electron and ion flows decouple. The first aim of this paper is to test whether or not this hypothesis can account for the scaling of the nonlinear reconnection rate reported in Ref. 10.

The second aim of this paper is to extend the investigation of Ref. 10 in order to determine the scaling of the maximum nonlinear Hall-MHD reconnection rate in the *high guide-field* limit. This limit is generally applicable to magnetic fusion experiments, whereas the opposite limit is more appropriate to astrophysical applications. In the high guide-field limit, the whistler wave is suppressed and magnetic reconnection is instead accelerated by the *kinetic Alfvén wave*.<sup>19</sup> Rogers *et al.*<sup>19</sup> report that the nonlinear reconnection rate in this limit is again *independent* of the mechanism by which magnetic-field lines are broken. On the other hand, Grasso *et al.*<sup>20</sup> report that the nonlinear reconnection rate *does* depend on the field-line breaking mechanism. We hope to establish which of these two results holds for the Taylor problem.

The numerical investigation of magnetic reconnection in the high guide-field limit is rendered particularly problematic by the severe time-step limit associated with the compressional Alfvén wave. This wave propagates very rapidly, but does not play a central role in the reconnection process. Hence, it is a standard practice to numerically evolve a “reduced” set of equations which exclude the compressional Alfvén wave. In this paper, we present a reduction scheme which yields a set of reduced equations valid in both the high and low guide-field limits. In comparison, the conventional reduction scheme yields equations which are only valid in the high guide-field limit.<sup>21</sup> Our reduced equations enable us to investigate forced magnetic reconnection with an arbitrary guide field using a single system of equations.

## II. DERIVATION OF REDUCED EQUATIONS

### A. Basic equations

Standard right-handed Cartesian coordinates  $(x, y, z)$  are adopted. It is assumed that there is no variation along the  $z$  axis, i.e.,  $\partial/\partial z \equiv 0$ .

Consider a magnetized, two-species (electron and ion), quasineutral plasma with singly charged ions of mass  $m_i$  and constant, uniform number density  $n_0$ . It is convenient to adopt a normalization scheme such that all lengths are measured in terms of some scale length  $a$ , all magnetic fields in terms of some scale field strength  $B_0$ , all velocities in terms of the characteristic Alfvén speed  $V_A = B_0 / \sqrt{\mu_0 n_0 m_i}$ , and all pressures in terms of  $B_0^2 / \mu_0$ . This normalization scheme is described in more detail in Ref. 10.

Writing the magnetic field in the form

$$\mathbf{B} = \nabla \psi \wedge \hat{\mathbf{z}} + B_z \hat{\mathbf{z}}, \quad (3)$$

the compressible Hall-MHD equations<sup>10,22</sup> reduce to

$$\frac{\partial \psi}{\partial t} = -\mathbf{V} \cdot \nabla \psi + d_i [\psi, B_z] + \eta \nabla^2 \psi, \quad (4)$$

$$\begin{aligned} \frac{\partial B_z}{\partial t} = & -\mathbf{V} \cdot \nabla B_z + d_i [\nabla^2 \psi, \psi] + [V_z, \psi] - B_z \nabla \cdot \mathbf{V} \\ & + \eta \nabla^2 B_z, \end{aligned} \quad (5)$$

$$\frac{\partial \mathbf{V}}{\partial t} = -(\mathbf{V} \cdot \nabla) \mathbf{V} - \nabla P - B_z \nabla B_z - \nabla^2 \psi \nabla \psi + \mu \nabla^2 \mathbf{V}, \quad (6)$$

$$\frac{\partial V_z}{\partial t} = -\mathbf{V} \cdot \nabla V_z + [B_z, \psi] + \mu \nabla^2 V_z, \quad (7)$$

$$\frac{\partial P}{\partial t} = -\mathbf{V} \cdot \nabla P - \Gamma P \nabla \cdot \mathbf{V} + \kappa \nabla^2 P, \quad (8)$$

where  $\mathbf{V}$  is the ion velocity in the  $x$ - $y$  plane,  $V_z$  the ion velocity along the  $z$  axis,  $P$  the plasma pressure,  $d_i = (c/\omega_{pi})/a$  the (normalized) collisionless ion skin depth,  $\eta$  the plasma resistivity (effectively, the inverse Lundquist number),  $\mu$  the plasma viscosity,  $\kappa$  the plasma heat conductivity,  $\Gamma = 5/3$  the ratio of specific heats, and  $[A, B] \equiv \nabla A \wedge \nabla B \cdot \hat{\mathbf{z}}$ . In deriving the above equations, we have neglected density variations, nonscalar pressure, and anisotropic transport. We have also adopted a cold ion ordering.

### B. Reduction scheme

Our reduction process is designed to eliminate the compressional Alfvén wave, which becomes increasingly difficult to handle numerically as the out-of-plane magnetic-field strength  $B_z$  rises, and only plays a significant role in the reconnection process for a period of a few Alfvén times after the onset of the boundary perturbation.<sup>23</sup> This general approach was first employed by Strauss.<sup>24</sup>

Let

$$P(x, y, t) = P^{(0)} + B^{(0)} p_1(x, y, t) + p_2(x, y, t), \quad (9)$$

$$B_z(x, y, t) = B^{(0)} + b_z(x, y, t). \quad (10)$$

Here,  $P^{(0)}$  and  $B^{(0)}$  are constants, whereas  $p_1$ ,  $p_2$ , and  $b_z$  are all  $O(1)$ . The fundamental ordering scheme adopted in our reduction process is

$$P^{(0)} \gg B^{(0)} \gg 1. \quad (11)$$

This scheme ensures that the compressional Alfvén wave propagates far more rapidly than any other wave in our system of equations, and hence effectively decouples from these other waves when the plasma motion is relatively slow.

On time scales much longer than the transit time for the compressional Alfvén wave, which is assumed to be effectively instantaneous, the plasma motion is almost *incompressible*. Hence, we can write

$$\mathbf{V} \approx \nabla \phi \wedge \hat{\mathbf{z}}. \quad (12)$$

Taking the curl of the  $\mathbf{V}$  equation, to lowest order our Hall-MHD equations (4)–(8) reduce to

$$\frac{\partial \psi}{\partial t} = [\phi, \psi] + d_i [\psi, b_z] + \eta \nabla^2 \psi, \tag{13}$$

$$\begin{aligned} \frac{\partial b_z}{\partial t} \simeq & [\phi, b_z] + d_i [\nabla^2 \psi, \psi] + [V_z, \psi] - B^{(0)} \nabla \cdot \mathbf{V} \\ & + \eta \nabla^2 b_z, \end{aligned} \tag{14}$$

$$\frac{\partial U}{\partial t} = [\phi, U] + [\nabla^2 \psi, \psi] + \mu \nabla^2 U, \tag{15}$$

$$\frac{\partial V_z}{\partial t} = [\phi, V_z] + [B_z, \psi] + \mu \nabla^2 V_z, \tag{16}$$

$$\frac{\partial p_1}{\partial t} \simeq [\phi, p_1] - \frac{\Gamma P^{(0)}}{B^{(0)}} \nabla \cdot \mathbf{V} + \kappa \nabla^2 p_1, \tag{17}$$

where  $U = \nabla^2 \phi$ . Note that  $\nabla \cdot \mathbf{V}$  cannot be neglected in Eqs. (14) and (17), since it is multiplied by the large factors  $B^{(0)}$  and  $\Gamma P^{(0)}/B^{(0)}$ , respectively.

To lowest order, we expect the compressional Alfvén wave to maintain approximate force balance within the plasma, provided that the plasma motion is sufficiently slow. In other words, to lowest order we expect Eq. (6) to imply

$$\nabla P \simeq -B_z \nabla B_z - \nabla^2 \psi \nabla \psi. \tag{18}$$

Applying our fundamental ordering scheme (11), we obtain

$$\nabla p_1 \simeq -\nabla b_z. \tag{19}$$

Finally,  $\nabla \cdot \mathbf{V}$  can be eliminated from Eqs. (14) and (17), making use of the above force balance equation, to yield our set of reduced equations:

$$\frac{\partial \psi}{\partial t} = [\phi, \psi] + d_\beta [\psi, Z] + \eta \nabla^2 \psi, \tag{20}$$

$$\frac{\partial Z}{\partial t} = [\phi, Z] + d_\beta [\nabla^2 \psi, \psi] + c_\beta [V_z, \psi] + \frac{(\kappa + \beta \eta)}{1 + \beta} \nabla^2 Z, \tag{21}$$

$$\frac{\partial U}{\partial t} = [\phi, U] + [\nabla^2 \psi, \psi] + \mu \nabla^2 U, \tag{22}$$

$$\frac{\partial V_z}{\partial t} = [\phi, V_z] + c_\beta [Z, \psi] + \mu \nabla^2 V_z, \tag{23}$$

where  $U = \nabla^2 \phi$ ,  $c_\beta = \sqrt{\beta/(1 + \beta)}$ ,  $d_\beta = c_\beta d_i$ , and  $Z = b_z/c_\beta$ . Here,

$$\beta = \frac{\Gamma P^{(0)}}{[B^{(0)}]^2} \tag{24}$$

is the conventional plasma beta parameter (multiplied by  $\Gamma$ ) calculated using the guide field  $B^{(0)}$ . Thus,  $\beta \gg 1$  corresponds to a low guide-field ordering, and *vice versa*. Note that our fundamental ordering scheme (11) does not constrain  $\beta$  to be either much less than or much greater than unity. The initial equilibrium associated with the above set of equations satisfies

$$p_2(x) + c_\beta^2 [Z(x)]^2 + [B_y(x)]^2 = \text{const}, \tag{25}$$

where  $B_y = -d\psi/dx$ . Note that Mirnov *et al.*<sup>25</sup> have independently performed similar analysis to the above in the linear regime.

### C. Zero guide-field limit

In the zero guide-field limit,  $B^{(0)} \rightarrow 0$ , which corresponds to  $\beta \rightarrow \infty$ , we adopt the modified ordering

$$P = P^{(0)} + p_1, \tag{26}$$

$$B_z = b_z, \tag{27}$$

where  $P^{(0)} \gg 1$  is a uniform constant and  $p_1, b_z$  are  $O(1)$ . As before, the purpose of this ordering scheme is to make the compressional Alfvén wave propagate much faster than any other wave in the system.

From Eq. (17), the above ordering scheme implies that  $\nabla \cdot \mathbf{V} = 0$ . In this limit, the remaining two-fluid equations readily yield Eqs. (20)–(23), with  $c_\beta = 1$  and  $d_\beta = d_i$ .

We conclude that Eqs. (20)–(23) hold in the zero, small, and large guide-field limits, as long as the compressional Alfvén wave propagates more rapidly than any other wave in the system.

### D. High- $\beta$ limit

In the high- $\beta$  (i.e., low guide-field) limit,  $\beta \gg 1$ , our reduced equations (20)–(23) simplify somewhat to give the following equations:

$$\frac{\partial \psi}{\partial t} = [\phi, \psi] + d_i [\psi, Z] + \eta \nabla^2 \psi, \tag{28}$$

$$\frac{\partial Z}{\partial t} = [\phi, Z] + d_i [\nabla^2 \psi, \psi] + [V_z, \psi] + \eta \nabla^2 Z, \tag{29}$$

$$\frac{\partial U}{\partial t} = [\phi, U] + [\nabla^2 \psi, \psi] + \mu \nabla^2 U, \tag{30}$$

$$\frac{\partial V_z}{\partial t} = [\phi, V_z] + [Z, \psi] + \mu \nabla^2 V_z, \tag{31}$$

where  $Z \simeq b_z$ . The above system of equations can be obtained directly from Eqs. (4)–(8) by assuming incompressible flow and a negligible guide field, i.e., negligible equilibrium  $B_z$ . As explained in Ref. 10 (and references therein), this system describes magnetic reconnection which proceeds at an accelerated rate (compared to resistive MHD) due to the action of the *whistler wave*.

### E. Low- $\beta$ limit

In the low- $\beta$  (i.e., high guide-field) limit,  $\beta \ll 1$ , our reduced equations (20)–(23) simplify somewhat to give the following equations:

$$\frac{\partial \psi}{\partial t} = [\phi, \psi] + \rho_s [\psi, Z] + \eta \nabla^2 \psi, \tag{32}$$

$$\frac{\partial Z}{\partial t} = [\phi, Z] + \rho_s [\nabla^2 \psi, \psi] + \sqrt{\beta} [V_z, \psi] + \kappa \nabla^2 Z, \tag{33}$$

$$\frac{\partial U}{\partial t} = [\phi, U] + [\nabla^2 \psi, \psi] + \mu \nabla^2 U, \quad (34)$$

$$\frac{\partial V_z}{\partial t} = [\phi, V_z] + \sqrt{\beta} [Z, \psi] + \mu \nabla^2 V_z, \quad (35)$$

where  $\rho_s = \sqrt{\beta} d_i$ . These are the familiar “four-field equations” first obtained by Hazeltine *et al.*<sup>21</sup> The four-field system describes magnetic reconnection which is accelerated by the kinetic Alfvén wave.<sup>26</sup>

### F. Zero- $\beta$ limit

In the zero- $\beta$  limit, with  $\beta=0$  but  $\rho_s$  finite, the four-field equations simplify further to give  $Z \approx \rho_s U$ , and

$$\frac{\partial \psi}{\partial t} = [\phi, \psi] + \rho_s^2 [\psi, U] + \eta \nabla^2 \psi, \quad (36)$$

$$\frac{\partial U}{\partial t} = [\phi, U] + [\nabla^2 \psi, \psi] + \mu \nabla^2 U. \quad (37)$$

These are the familiar “two-field” equations used by Grasso and co-workers to investigate kinetic Alfvén wave accelerated magnetic reconnection.<sup>20</sup>

### G. Discussion

Using a standard reduction process designed to eliminate the compressional Alfvén wave, we have derived a set of four reduced equations (20)–(23), which describe Hall-MHD magnetic reconnection in two dimensions. The important feature of these equations is that they contain *both* the whistler wave *and* the kinetic Alfvén wave. Although these two waves are thought to play similar roles in the reconnection process, hitherto they have only been studied separately using different sets of equations.<sup>19</sup>

## III. SETTING UP THE TAYLOR PROBLEM

### A. Plasma equilibrium

Suppose that the plasma is bounded by perfectly conducting walls located at  $x = \pm 1$  and is periodic in the  $y$  direction with periodicity length  $L$ . The initial plasma equilibrium satisfies

$$\psi^{(0)}(x) = -\frac{x^2}{2}, \quad (38)$$

and  $Z^{(0)}(x) = \phi^{(0)}(x) = U^{(0)}(x) = V_z^{(0)}(x) = 0$ . In unnormalized units,  $B_0$  is the equilibrium magnetic-field strength in the  $x$ - $y$  plane measured at  $|x|=a$  and  $a$  is half the distance between the conducting walls. Note that the above plasma equilibrium is *completely stable* to tearing modes.

### B. Boundary conditions

Suppose that the conducting wall at  $x=1$  is subject to a *small* (compared with unity) displacement  $\Xi(t) \sin(ky)$  in the  $x$  direction, where  $k = 2\pi/L$ . An equal and opposite displacement is applied to the wall at  $x=-1$ . The appropriate boundary conditions at the walls are the following:

$$\psi(\pm 1, y, t) = -\frac{1}{2} + \Xi(t) \sin(ky), \quad (39)$$

$$Z(\pm 1, y, t) = 0, \quad (40)$$

$$\phi(\pm 1, y, t) = \mp \frac{1}{k} \frac{d\Xi(t)}{dt} \cos(ky), \quad (41)$$

$$U(\pm 1, y, t) = 0, \quad (42)$$

$$V_z(\pm 1, y, t) = 0. \quad (43)$$

Let

$$\Xi(t) = \Xi_0 [1 - e^{-t/\tau} - (t/\tau) e^{-t/\tau}] \quad (44)$$

for  $t \geq 0$ , with  $\Xi(t) = 0$  for  $t < 0$ . Note that both  $\Xi(t)$  and  $d\Xi(t)/dt$  are continuous at  $t=0$ , and  $\Xi(t) \rightarrow \Xi_0$  as  $t \rightarrow \infty$ . All fields are assumed to be unperturbed at  $t=0$ .

### C. Reconnection diagnostics

The magnetic  $O$  and  $X$  points are located at  $(x, y) = (0, L/4)$  and  $(0, 3L/4)$ , respectively. The *reconnected magnetic flux* is written as

$$\Psi(t) = \frac{1}{2} [\psi(X \text{ point}) - \psi(O \text{ point})], \quad (45)$$

whereas the *magnetic reconnection rate* is defined as

$$R(t) = \frac{d\Psi(t)}{dt}. \quad (46)$$

## IV. NUMERICAL RESULTS

### A. Introduction

Equations (20)–(23), plus the initial equilibrium described in Sec. III A and the boundary conditions (39)–(43), have been implemented numerically in a finite-difference code which is second order in both space and time. As described in Ref. 10, a phenomenological fourth-order diffusion, or “hyperresistivity,” term is added to Eqs. (20) and (21) for numerical reasons. The code makes use of a semi-implicit algorithm modeled after that of Harned and Mikic<sup>27</sup> in order to circumvent the highly restrictive Courant–Freidrichs–Lewy condition on the whistler/kinetic-Alfvén wave. The computational grid is uniform in the  $y$  direction. However, in order to help resolve the reconnecting region, the grid points in the  $x$  direction are more closely packed in the vicinity of the magnetic resonance. All of the simulations discussed in this paper employ a uniform time step of  $\delta t = 10^{-3}$  normalized time units, as well as a  $256 \times 128$  computational grid. The hyperresistivity is set to  $\nu = 2.5 \times 10^{-9}$ , which is large enough to maintain numerical stability, but not so large as to significantly affect the peak reconnection rate.<sup>10</sup> The parameters  $\mu$  and  $\kappa$  are both set to the extremely low value  $10^{-7}$ , and are, thus, not expected to play an important role in the reconnection process.

### B. Overview

Figure 1 shows the magnetic reconnection rate versus time for a pair of calculations in the nonlinear Hall-MHD regime. The two calculations are identical apart from the magnitude of the guide field: one is performed in the low guide-field limit ( $\beta \gg 1$ ), whereas the other is performed in

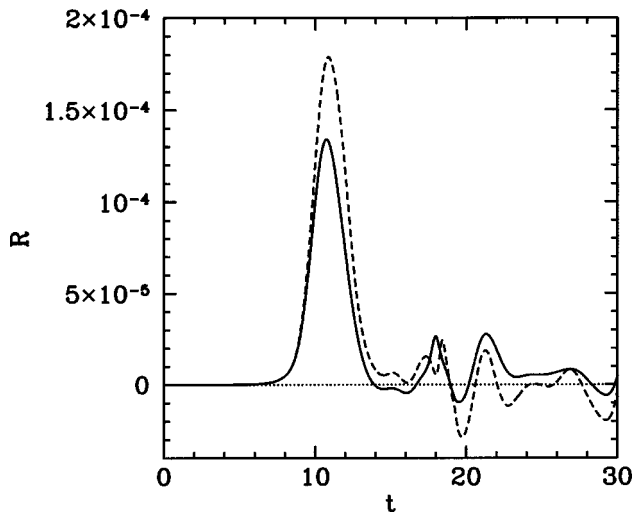


FIG. 1. The magnetic reconnection rate  $R$  vs time in the nonlinear Hall-MHD regime. Calculations performed with  $L=8.0$ ,  $\tau=1.0$ ,  $\eta=10^{-6}$ ,  $\mu=10^{-7}$ ,  $\kappa=10^{-7}$ ,  $d_\beta=0.5$ , and  $\Xi_0=10^{-2}$ . The solid curve corresponds to  $\beta=10^2$  and the dashed curve corresponds to  $\beta=10^{-2}$ .

the high guide-field limit ( $\beta \ll 1$ ). In contrast, Fig. 2 shows the magnetic reconnection rate versus time for a calculation in the nonlinear resistive-MHD regime. The parameters for this calculation are the same as those for the calculations shown in Fig. 1, except that the collisionless ion skin depth is set to zero. Note that the value of  $\beta$  is immaterial in Fig. 2, since the guide field has no effect on the reconnection rate in the resistive-MHD regime.

An examination of Figs. 1 and 2 reveals a number of interesting features of nonlinear Hall-MHD magnetic reconnection. First, and most obviously, Hall effects *greatly increase* the reconnection rate compared to that obtained in the resistive-MHD regime. Indeed, the peak reconnection rate shown in Fig. 1 is about 30 times that shown in Fig. 2.

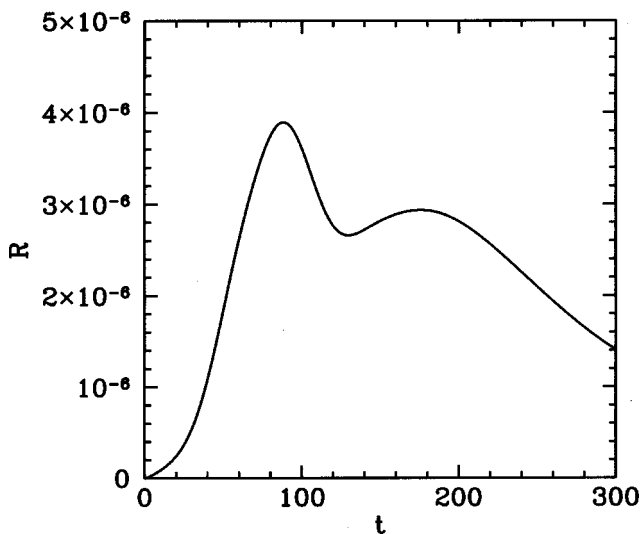


FIG. 2. The magnetic reconnection rate  $R$  vs time in the nonlinear resistive-MHD regime. Calculations performed with  $L=8.0$ ,  $\tau=1.0$ ,  $\eta=10^{-6}$ ,  $\mu=10^{-7}$ ,  $\kappa=10^{-7}$ ,  $d_\beta=0.0$ , and  $\Xi_0=10^{-2}$ .

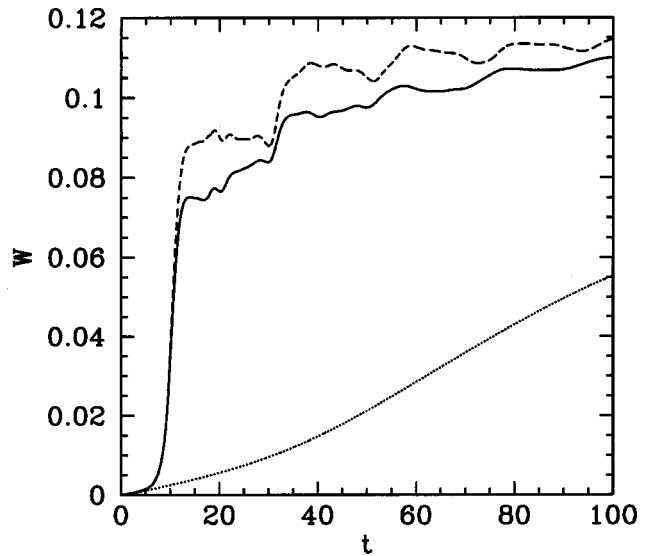


FIG. 3. The full island width  $W$  vs time. Calculations performed with  $L=8.0$ ,  $\tau=1.0$ ,  $\eta=10^{-6}$ ,  $\mu=10^{-7}$ ,  $\kappa=10^{-7}$ , and  $\Xi_0=10^{-2}$ . The solid curve corresponds to  $d_\beta=0.5$  and  $\beta=10^2$ . The dashed curve corresponds to  $d_\beta=0.5$  and  $\beta=10^{-2}$ . The dotted curve corresponds to  $d_\beta=0.0$ .

Second, Hall-MHD reconnection is far more *impulsive* in nature than resistive-MHD reconnection. For instance, in Fig. 1 there is initially very little response to the applied boundary perturbation. However, about eight Alfvén times after the onset of the perturbation the reconnection rate suddenly rises precipitously. Conversely, in Fig. 2 the onset of driven reconnection is fairly gradual in nature. Note, also, that in Fig. 1 the reconnection rate drops rapidly to a relatively low and rather unsteady value after the initial surge of reconnection. By contrast, in Fig. 2 the reconnection rate falls far more slowly after attaining its peak value.

Third, it can be seen from Fig. 1 that the reconnection rate in the Hall-MHD regime is *fairly insensitive* to the guide-field parameter  $\beta$ , provided that the collisionless ion skin-depth parameter  $d_\beta = \sqrt{\beta/(1+\beta)}d_i$  remains fixed. Note that the two calculations shown in Fig. 1 have  $\beta$  values differing by four orders of magnitude. Nevertheless, the two reconnection rate curves are fairly similar, especially during the initial surge of reconnection, with the high-guide field (low- $\beta$ ) case reconnecting slightly faster.

Figure 3 shows the full magnetic island width  $W = 4\sqrt{\Psi}$  versus time for the three calculations displayed in Figs. 1 and 2. Note that the theoretical final saturated island width in all three cases is  $W_0 \approx 0.347$ . We can make the following observations. In the nonlinear Hall-MHD regime, there is an initial surge of fast reconnection during which the island grows substantially, achieving about 25% of its final width, followed by a period of much slower unsteady growth that eventually asymptotes to conventional Rutherford<sup>28</sup> growth (which takes place on a resistive time scale). In the nonlinear resistive-MHD regime, the island growth also eventually asymptotes to Rutherford growth, but there is no initial surge of fast reconnection.

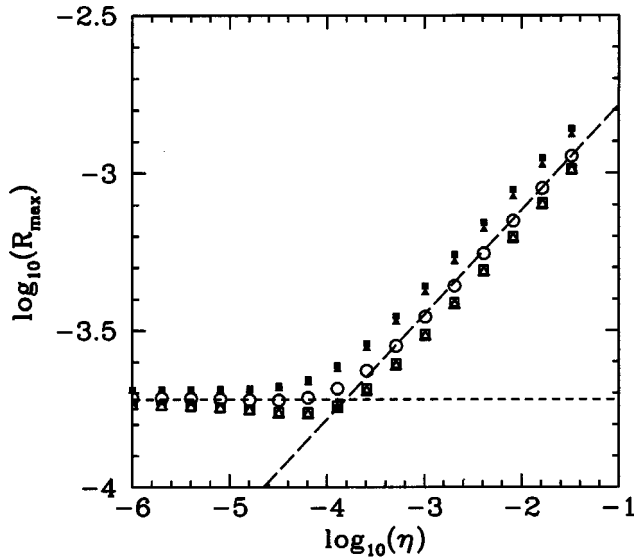


FIG. 4. Scaling of the peak magnetic reconnection rate  $R_{\max}$  with the resistivity  $\eta$  for various values of  $\beta$ . Calculations performed with  $L=8.0$ ,  $\tau=1.0$ ,  $\mu=10^{-7}$ ,  $\kappa=10^{-7}$ ,  $d_\beta=1.0$ , and  $\Xi_0=10^{-2}$ . The open triangular data points correspond to  $\beta=10^2$ . The open square data points corresponds to  $\beta=10^1$ . The open circular data points correspond to  $\beta=10^0$ . The solid triangular data points correspond to  $\beta=10^{-1}$ . The solid square data points correspond to  $\beta=10^{-2}$ . The short-dashed line is a fit to  $R_{\max} \propto \eta^0$ . The long-dashed line is a fit to  $R_{\max} \propto \eta^{1/3}$ .

### C. Scaling of the peak reconnection rate

This section examines the scaling of the *peak* magnetic reconnection rate  $R_{\max}$  in the nonlinear Hall-MHD regime, with the resistivity  $\eta$ , the amplitude of the boundary perturbation,  $\Xi_0$ , the collisionless ion skin-depth parameter  $d_\beta$ , and the guide-field parameter  $\beta$ . Note that the reconnection rate is a direct measure of the inductive *electric field* generated in the reconnecting region. The electric field is, of course, responsible for *particle acceleration*, which is generally the most important byproduct of magnetic reconnection. Hence, the peak reconnection rate is a sensible metric to choose in order to characterize the reconnection process, since it essentially measures the strength of the accompanying particle acceleration. This is especially the case for nonlinear Hall-MHD reconnection in the Taylor problem, because, as is apparent from Figs. 1 and 3, the reconnection rate is *extremely sharply peaked* in time. In this situation, we would clearly expect virtually all of the particle acceleration to take place during the initial surge of fast reconnection, with the strength of the acceleration being closely related to the peak reconnection rate during this surge. Note also that a significant amount of island growth, and associated release of magnetic energy, takes place during the initial reconnection surge.

Figure 4 shows the scaling of the peak reconnection rate  $R_{\max}$  with resistivity  $\eta$  keeping all other parameters (except  $\beta$ ) fixed. Data are shown for various widely differing values of the guide-field parameter  $\beta$ . Note that as  $\beta$  is varied the parameter  $d_\beta$ , rather than  $d_i$ , is held constant. It can be seen that when  $\eta$  is relatively large the reconnection rate scales as  $\eta^{1/3}$ . This is a linear scaling—see Ref. 10. However, as  $\eta$  is decreased the system eventually enters the nonlinear regime.

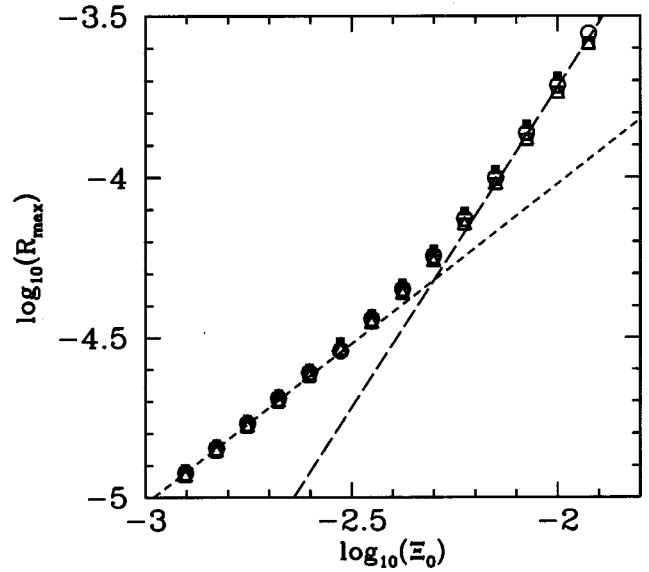


FIG. 5. Scaling of the peak magnetic reconnection rate  $R_{\max}$ , with the boundary perturbation amplitude  $\Xi_0$ , for various values of  $\beta$ . Calculations performed with  $L=8.0$ ,  $\tau=1.0$ ,  $\eta=10^{-6}$ ,  $\mu=10^{-7}$ ,  $\kappa=10^{-7}$ , and  $d_\beta=1.0$ . The data points are as described in the caption to Fig. 4. The short-dashed line is a fit to  $R_{\max} \propto \Xi_0^1$ . The long-dashed line is a fit to  $R_{\max} \propto \Xi_0^2$ .

In this regime, the reconnection rate clearly becomes independent of  $\eta$ . Note that the scaling of the reconnection rate is the same for all values of  $\beta$ , both large and small. However, the reconnection rate does rise slightly as  $\beta$  decreases.

Figure 5 shows the scaling of the peak reconnection rate  $R_{\max}$  with boundary perturbation amplitude  $\Xi_0$ , keeping all other parameters (except  $\beta$ ) fixed. It can be seen that when  $\Xi_0$  is relatively small the reconnection rate scales as  $\Xi_0^1$ . This is again a linear scaling—see Ref. 10. However, as  $\Xi_0$  is increased the system eventually enters the nonlinear regime. In this regime, the reconnection rate scales approximately as  $\Xi_0^2$ . Note, again, that the scaling of the reconnection rate is the same for all  $\beta$  values, with the reconnection rate being slightly higher at small  $\beta$ .

Figure 6 shows the scaling of the peak reconnection rate  $R_{\max}$  with the collisionless ion skin-depth parameter  $d_\beta$ , keeping all other parameters (except  $\beta$ ) fixed. It can be seen that when  $d_\beta$  is relatively small the reconnection rate is independent of  $d_\beta$ . This is a resistive-MHD result—see Ref. 10. However, as  $d_\beta$  is increased the system eventually enters the Hall-MHD regime. In this regime, the reconnection rate scales approximately as  $d_\beta^{3/2}$ . However, this scaling breaks down as  $d_\beta$  approaches the system size (i.e.,  $d_\beta \rightarrow 1$ ). Note, again, that the scaling of the reconnection rate is the same for all  $\beta$  values, with the reconnection rate being slightly higher at small  $\beta$ .

It follows from Figs. 4–6 that the peak reconnection rate in the nonlinear Hall-MHD regime with arbitrary guide field scales approximately as

$$R_{\max} \sim d_\beta^{3/2} \Xi_0^2, \tag{47}$$

provided  $d_\beta$  remains significantly less than the system size. In the above formula, we have neglected the relatively weak scaling with  $\beta$  when the parameter  $d_\beta$  is held constant.

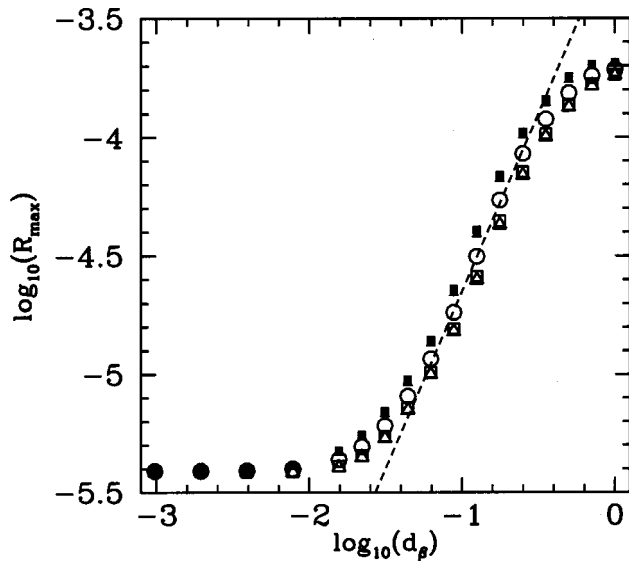


FIG. 6. Scaling of the peak magnetic reconnection rate  $R_{\max}$ , with the collisionless ion skin-depth parameter  $d_\beta$ , for various values of  $\beta$ . Calculations performed with  $L=8.0$ ,  $\tau=1.0$ ,  $\eta=10^{-6}$ ,  $\mu=10^{-7}$ ,  $\kappa=10^{-7}$ , and  $\Xi_0=10^{-2}$ . The data points are as described in the caption to Fig. 4. The short-dashed line is a fit to  $R_{\max} \propto d_\beta^{3/2}$ .

Shay *et al.* have advanced a theory of nonlinear two-fluid magnetic reconnection which depends crucially on a parameter known as the upstream magnetic-field strength.<sup>18</sup> This is the magnitude of the reconnecting field evaluated at the edge of the dissipation region, i.e., the region surrounding the resonant surface where resistive MHD breaks down. According to Shay *et al.*, the reconnection rate should be directly proportional to the upstream field strength. Unfortunately, this quantity is very difficult to evaluate in the Taylor problem. In all of our Hall-MHD simulations, we observe that even a long way from the resonant surface the plasma exhibits significant oscillations between the ion and electron flows on the  $d_\beta$  scale, and is, thus, not very well described by resistive MHD. Incidentally, such oscillations were first predicted by Mahajan and Yoshida.<sup>29</sup> We can (somewhat arbitrarily) attempt to define the width of the dissipation region,  $\delta$ , as the distance between the  $X$  point and the first zero of the ion current (measured on a straight line which runs perpendicular to the resonant surface and passes through the  $X$  point). Using this definition, we find that  $\delta$  (evaluated at the time of the peak reconnection rate) is proportional to  $d_\beta$  but shows very little scaling with either  $\Xi_0$  or  $\eta$ . Now, the upstream magnetic-field strength is directly proportional to  $\delta$ , since we find that the reconnecting magnetic field always varies roughly linearly (with  $x$ ) across the dissipation region, even in the nonlinear regime. Hence, according to Shay *et al.*,<sup>18</sup> the scaling of the maximum reconnection rate should be  $R_{\max} \sim d_\beta$ . However, we instead obtain  $R_{\max} \sim d_\beta^{3/2} \Xi_0^2$ . We conclude that the Shay model *cannot* account for the scaling of the reconnection rate in the nonlinear Hall-MHD Taylor problem. In particular, this model is quite unable to account for the observed strong variation of the reconnection rate with the amplitude of the boundary perturbation.

Shay *et al.* have recently suggested<sup>30</sup> that their general

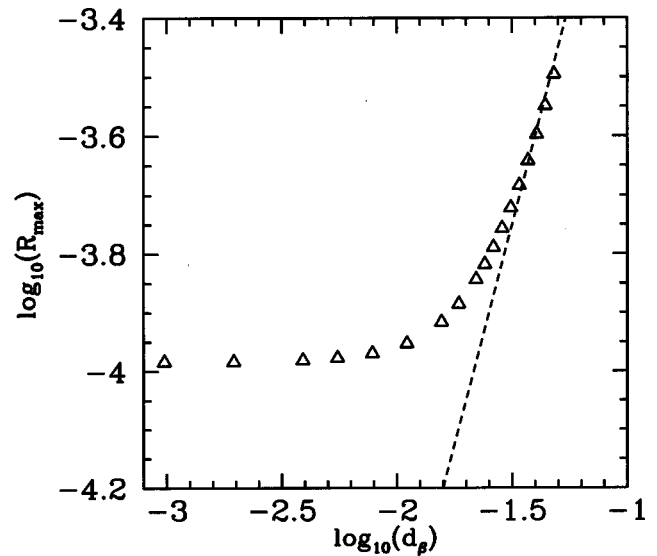


FIG. 7. Scaling of the peak magnetic reconnection rate  $R_{\max}$ , with the collisionless ion skin-depth parameter  $d_\beta$ . Calculations performed with  $L=8.0$ ,  $\tau=1.0$ ,  $\eta=10^{-6}$ ,  $\mu=10^{-7}$ ,  $\kappa=10^{-7}$ ,  $\Xi_0=10^{-1}$ , and  $\beta=10^2$ . The short-dashed line is a fit to  $R_{\max} \propto d_\beta^{3/2}$ .

theory is only applicable when the collisionless ion skin depth  $d_i$  is much less than the island width  $W$ . This is certainly not the case for any of the calculations described in this paper so far, which may account for the Shay model's lack of success. Figure 7 shows the scaling of the maximum magnetic reconnection rate  $R_{\max}$ , with the collisionless ion skin-depth parameter  $d_\beta$  (which in this case is virtually identical to  $d_i$ ), for a set of calculations in which the ratio  $W/d_\beta$  is made as large as practically possible. In fact, in these calculations  $W/d_\beta \sim 10$  in the nonlinear Hall-MHD regime, at the end of the initial surge of fast reconnection. It can be seen that the data shown in Fig. 7 are consistent with an asymptotic  $R_{\max} \sim d_\beta^{3/2}$  scaling, although the exact asymptotic scaling with  $d_\beta$  is difficult to determine with any accuracy. Certainly, a comparison of Figs. 6 and 7 would not appear to indicate that the  $d_\beta$  scaling in the  $W/d_\beta \gg 1$  regime is radically different from that in the  $W/d_\beta \ll 1$  regime. Moreover, the previously mentioned strong scaling of the peak reconnection rate with the perturbation amplitude persists in the  $W/d_\beta \gg 1$  regime. These facts cast further doubt on the applicability of the Shay model to the Taylor problem, even in the limit  $W/d_\beta \gg 1$ .

## V. SUMMARY AND DISCUSSION

We have derived a set of reduced equations (20)–(23), which describe Hall-MHD magnetic reconnection in two dimensions. These equations contain both the whistler wave and the kinetic Alfvén wave, and are valid for arbitrary guide-field strength. At present, our equations neglect electron inertia and ion pressure. However, adding these effects would be a fairly straightforward exercise. Using our equations, we have investigated the scaling of the rate of driven magnetic reconnection in the Taylor problem. In this problem, a small amplitude boundary perturbation is suddenly



applied to a tearing stable, slab plasma equilibrium. The perturbation is such as to drive magnetic reconnection within the plasma.

We find that in the nonlinear Hall-MHD regime with arbitrary guide field the peak reconnection rate  $R_{\max}$  scales approximately as

$$R_{\max} \sim \left( \frac{\beta}{1+\beta} \right)^{3/4} d_i^{3/2} \Xi_0^2, \quad (48)$$

where  $\beta$  is the plasma beta calculated using the guide field,  $d_i$  the collisionless ion skin depth, and  $\Xi_0$  the amplitude of the external perturbation. This scaling is a generalization of the low guide-field (i.e.,  $\beta \gg 1$ ) scaling reported in Ref. 10. We find that the above scaling cannot be accounted for in terms of the general theory proposed by Shay *et al.*<sup>18</sup> Note that the peak reconnection rate has no dependence on the mechanism by which magnetic-field lines are broken (i.e., on the resistivity). This is true for all values of the guide field.

## ACKNOWLEDGMENTS

The author gratefully acknowledges helpful discussions with Paul Watson, Mike Shay, Jim Drake, Barrett Rogers, Amitava Bhattacharjee, Vladimir Mirnov, and Franco Porcelli during the preparation of this paper.

This research was funded by the U.S. Department of Energy under Contract No. DE-FG05-96ER-54346 as well as via Cooperative Grant No. DE-FC02-01ER-54652 under the auspices of the program for Scientific Discovery through Advanced Computing (SIDAC).

<sup>1</sup>F. L. Waelbroeck, Phys. Fluids B **1**, 2372 (1989).

<sup>2</sup>K. Shibata, Adv. Space Res. **17**, 9 (1996).

<sup>3</sup>D. N. Baker, J. Geophys. Res. **101**, 12975 (1996).

<sup>4</sup>D. Biskamp, Phys. Fluids **29**, 1520 (1986).

<sup>5</sup>B. Coppi, Phys. Rev. Lett. **11**, 226 (1964).

<sup>6</sup>M. Ottaviani and F. Porcelli, Phys. Rev. Lett. **71**, 3802 (1993).

<sup>7</sup>T. S. Hahm and R. M. Kulsrud, Phys. Fluids **28**, 2412 (1985).

<sup>8</sup>X. Wang and A. Bhattacharjee, Phys. Fluids B **4**, 1795 (1992).

<sup>9</sup>R. Fitzpatrick, Phys. Plasmas **10**, 1782 (2003).

<sup>10</sup>R. Fitzpatrick, Phys. Plasmas **11**, 937 (2004).

<sup>11</sup>P. A. Sweet, *Electromagnetic Phenomena in Cosmical Physics* (Cambridge University Press, New York, NY, 1958).

<sup>12</sup>E. N. Parker, J. Geophys. Res. **62**, 509 (1957).

<sup>13</sup>D. Biskamp, E. Schwarz, and J. F. Drake, Phys. Rev. Lett. **75**, 3850 (1995).

<sup>14</sup>M. A. Shay, J. F. Drake, and B. N. Rogers, J. Geophys. Res. **106**, 3759 (2001).

<sup>15</sup>X. Wang, A. Bhattacharjee, and Z. W. Ma, Phys. Rev. Lett. **87**, 265003 (2001).

<sup>16</sup>W. H. Matthaeus (private communication).

<sup>17</sup>M. A. Shay, J. F. Drake, B. N. Rogers, and R. E. Denton, Geophys. Res. Lett. **26**, 2163 (1999).

<sup>18</sup>M. A. Shay, J. F. Drake, B. N. Rogers, and M. Swisdak, Bull. Am. Phys. Soc. **48**, 7 (2003).

<sup>19</sup>B. N. Rogers, R. E. Denton, J. F. Drake, and M. A. Shay, Phys. Rev. Lett. **87**, 195004 (2001).

<sup>20</sup>D. Grasso, F. Pegoraro, F. Porcelli, and F. Califano, Plasma Phys. Controlled Fusion **41**, 1497 (1999).

<sup>21</sup>R. D. Hazeltine, M. Kotschenreuther, and P. G. Morrison, Phys. Fluids **28**, 2466 (1985).

<sup>22</sup>S. I. Braginskii, *Reviews of Plasma Physics* (Consultants Bureau, New York, NY, 1965), Vol. 1, p. 205.

<sup>23</sup>R. Fitzpatrick, A. Bhattacharjee, Z. W. Ma, and T. Linde, Phys. Plasmas **10**, 4284 (2003).

<sup>24</sup>H. R. Strauss, Phys. Fluids **20**, 1354 (1977).

<sup>25</sup>V. V. Mirnov, C. C. Hegna, and S. C. Prager, Physics of Plasmas (submitted).

<sup>26</sup>A. Aydemir, Phys. Fluids B **4**, 3469 (1992).

<sup>27</sup>D. S. Harned and Z. Mikic, J. Comput. Phys. **83**, 1 (1989).

<sup>28</sup>P. Rutherford, Phys. Fluids **16**, 1903 (1973).

<sup>29</sup>S. M. Mahajan and Z. Yoshida, Phys. Rev. Lett. **81**, 4863 (1998).

<sup>30</sup>M. A. Shay, J. F. Drake, M. Swisdak, and B. N. Rogers, Phys. Plasmas **11**, 2199 (2004).